CELLULOSE ACETATE FIBERS WITH FLUORESCING NANOPARTICLES FOR ANTI-COUNTERFEITING PURPOSES

A Thesis

Presented to the Faculty of the Graduate School

of Cornell University

In Partial Fulfillment of the Requirements for the Degree of

Master of Science

by

Erin Sue Hendrick

August 2008

ABSTRACT

This research concerns the incorporation of fluorescent nanoparticles into cellulose acetate (CA) fibers. The resulting fibers that appear to be white until exposed to a certain frequency of light. The target application for these nanoparticle-containing fibers and fabrics is in anti-counterfeiting technology for documents, currency and apparel. The fluorescing nanoparticles used in this study, Cornell dots (C dots), have a fluorescent dye-containing silica core surrounded by a silica shell. The fluorescence of these nanoparticles can be tuned to a specific wavelength between 350 and 800 nm. The reproduction of this fluorescence at a precise wavelength, for several different wavelengths in a fiber pattern, would be difficult for counterfeiters to duplicate. A solution of CA and C dots was spun into a non-woven fabric using electrospinning, while single fibers were spun using dry spinning techniques. The actual weight percent of nanoparticles spun into these fibers was verified using thermogravimetric analysis (TGA). The C dot containing non-woven fabrics and fibers were then characterized using scanning electron microscopy (SEM) and confocal microscopy. The tensile properties of the fabrics and fibers were tested using ASTM standards for textiles to assess the effect that C dot loading had on the mechanical properties of the nonwoven fabrics and fibers.

BIOGRAPHICAL SKETCH

Erin S. Hendrick, a native of Rochester, NY, holds a Magna Cum Laude B.S. degree in Materials Science and Engineering from Alfred University.

ACKNOWLEDGMENTS

Special thanks to Margaret Frey, Chunhui Xiang, Min Xiao, and Mary Rebovich for all of their support. From the MS&E department, I would to thank Ulrich Wiesner and Erik Herz for their enthusiasm and advice. Additionally, I would like to recognize Carol Bayles and John Hunt for their guidance and assistance.

TABLE OF CONTENTS

LIST OF FIGURES

LIST OF TABLES

INTRODUCTION

Counterfeiting is a worldwide problem that results in the economic loss of hundreds of millions of dollars each year. Both consumers and producers are negatively affected by the influx of counterfeit items into the market. Corporations that produce commonly counterfeited items lose millions of dollars in revenue. For consumers, the presence of these counterfeit items increases the risk of purchasing faulty or poor quality products in place of legitimate ones. Commonly counterfeited items include clothing, documents and currency [1]. The International Chamber of Commerce has estimated that 7% of world trade is in counterfeit goods, approximately $350 million [2].

To counteract this problem, anti-counterfeiting technology is constantly being developed and improved. This technology seeks to mark authentic items in a way that is very difficult, hopefully impossible, to duplicate. However, due to the significant amount of total global trade that is amassed in counterfeit goods, the producers of these items are willing to spend considerable funds in order to keep up with these anti-counterfeiting methods[3]. Due to this challenge, new and better anti-counterfeiting technology is constantly in demand. Specifically, anti-counterfeiting technology is desired that is very difficult for counterfeiters to duplicate, and easy for users to positively identify.

Currently, much research has been done on the addition of a unique signal to polymeric materials. The types of signals imparted to these materials include fluorescence, magnetic, electrical, thermal, chemical, and radio frequency signals [4-16].

Fluorescence is conventionally applied to fibers using fluorescent dyes and coatings. Small fluorescent dye molecules can be placed in solution with dry polymer and solvent, which can then be spun into fibers. These dyes have the potential to leak

in certain environments, and to lose their strength during exposure to certain wavelengths of light. Common fluorescent dye molecules include Alq3, 10-(3-sulfopropyl), acridinium betaine, quinacrine dihydrochloride, naphthofluorescein, fluorescein, 8-hydroxypyrene-1, 3, 6-trisulfonic acid trisodium salt [4, 5]. These dyes can easily provide fluorescence to polymer fibers, but they are not permanent, and their volatile nature within fibers can lead to certain health and environmental concerns.

Therefore, though it is relatively simple to create fluorescent signal in fibers with fluorescent dyes, it is advisable to use a more contained method if longer-term fluorescence is desired. One way this can be accomplished is by using nanoparticles to coat the surface of a polymer fiber. Quantum dots are semiconductor-containing nanoparticles that can be used to produce color in fibers. These nanoparticles are relatively stable, last longer than conventional dye molecules, and can be applied to a fiber as a thin film coating [6].

Magnetic signals can be imparted to polymer fibers through polymer coatings that contain magnetic properties. These coatings can come in the form of composite materials, as well as magnetic nanoparticles embedded or coated onto polymer matrices. Traditionally, composite coatings have been applied to optical fiber, but they can be used to coat polymer fibers [7]. These magnetic coatings are composed of a polymer with an additional magnetic component. The research performed by Radojevic, et al. used the polymer poly(ethylene-co-vinyl acetate), with the magnetic powder $SmCo_5$. This coating was then applied to a glass or polymer fiber, giving the fiber a magnetic signal. Another method for creating magnetic fibers is through the use of magnetic nanoparticles. Electrospinning is an effective method for the creation of micro and nano-scale fibers from polymer materials. Magnetic nanoparticles can be dispersed in a polymer solution, and spun to form fiber mats. In one study by

Xianfeng et al., the polymer poly(vinyl pyrolidone) and magnetic PbS nanoparticles were electrospun together [8]. The researchers found this to be successful method for creating a fabric with magnetic signals.

In some cases, fibers can be used to measure thermal signal, rather than emit such a signal themselves. For example, Bayindir et al. have developed a fiber material that senses heat, and exhibits an electrical signal in response [9]. This device doesn't require optical probing signals, as is used in most other thermal-sensing devices. The fibers are thermally drawn, so the materials used have differing thermal and electrical properties: semiconducting, insulating, and metallic. Polymers that contain a thermal signal can be created with a combination of nanoporous polymer matrices, and nanoparticles that possess thermal properties [10]. As this is a patented approach, the inventors were not specific as to the polymer and nanoparticles used. However, it is known that the polymer can be used as an optical medium with tunable thermal properties. Such a polymer would be useful in optical fiber coatings because it can exhibit variable coefficients of thermal expansion (CTE), thermal conductivity, and thermo-optic coefficients.

Research into electrically conductive polymers has also become increasingly desirable for a large number of end-uses [5, 11-12]. More traditional conducting materials, such as metals, can be more expensive when lightweight complex shapes are desired. For this reason, polymeric materials with an electrical signal are desirable. Very few polymers exhibit the high conductivity seen in metals. However, by adding a certain dopant to a host polymer, metal-like electrical conductivity can be observed in certain polymers. For example, Moreda et al. have found that the addition of fluorine-containing peroxide is useful as a dopant in increasing the specific conductivity of polyacetylene [5]. Such an addition results in a polymer that exhibits semiconductor

level conductivity. Additionally, this dopant can give polyacetylene the level of conductivity observed in metals at very low temperatures.

Electrical signal can also be seen in entire fabrics. Researchers at North Carolina State University have developed woven electrical circuits that are formed through the interlacing of conducting and non-conducting threads [11]. The conducting threads carry the electric signal, while the non-conducting threads act as space-holders. These conducting threads are composed of polyester, with inter-dispersed threads of steel and copper threads. Such a fabric assembly can be attached to an electrical circuit, creating a fabric that can sense, actuate, communicate, and compute. This kind of conducting fiber is desirable for certain commercial applications, such as: power lines, antennas, and airbag wiring. NASA scientists use traditional fibers with a metallized coating to reduce cost for maintaining planes, military aircraft, and wires for missile guides [12]. Currently, there is high demand for "electro-textiles" in today's market, newer and more efficient methods for conducting fibers are continuously in demand.

In recent years, progress has been made on the integration of electrical components into various fabrics. In more recent developments, it was found that a chemical sensing component can be used in various fabrics to monitor the wearer's health and environment. This innovation functions through the interactions of an active surface and an integrated chemical sensor [13]. The biotechnology company, Biotex, has created a sensor that involves an inherently conducting polymer with some measure of fluid control. In this way, Biotex has created a textile substrate sensor that can monitor body fluids. The major application goal for the company is in textile substrates that can be used to monitor the pH of sweat through a color change [14]. This technology could someday be used to evaluate sports training and performance, as well as healthcare workers and hospitalized patients. Another company, CrossID, has developed a method for the application of a chemical signal to fibers for anti-

counterfeiting purposes. The system uses chemical particles with varying degrees of magnetism that emit a distinct radio frequency that can only be identified by a specific reader [15]. In this way, chemical and radio frequency signals can be combined to provide an effective anti-counterfeiting technique.

Radio frequency identification (RFID) tags are commonly applied to many products for identification using radio waves. Current technology is moving towards discrete RFID tags, or chipless RFID, which are more cost effective. Chipless RF fibers, which contain fibers that reflect and return a unique signal as an identifier, are currently under investigation [16]. These fibers are normally thin threads or fine wires, and can be applied to a container or garment in the same manner as traditional RFID tags.

As can be seen, an abundance of research has been performed on the addition of specific signals to polymeric materials. Though these signals serve a variety of purposes, the addition of unique signals into polymers for anti-counterfeit technology is especially intriguing. The sizeable amount of research on this topic confirms that new and effective anti-counterfeiting devices are constantly in demand. Therefore, this project has the potential to impart significant advances in this field. This research focuses on the creation of an anti-counterfeit device using Cornell dots, which impart a unique fluorescence signal, and cellulose acetate fibers.

Ulrich Wiesner and Hooisweng Ow developed Cornell dots, or C dots, in the Materials Science and Engineering department at Cornell University [17]. These nanoparticles are composed of a 2.2 nm fluorescent dye core surrounded by a silica shell that exhibits color when excited by an external light source at a specific wavelength. The C dots are 20-30 times brighter than single fluorescent dye molecules, and exhibit greater resistance to photo bleaching [18]. The silica shell allows the particles to maintain brightness for longer than a fluorescent solution

(Figure 1). These nanoparticles can be dispersed in several different solvents, including water and acetone, without degradation. To disperse the C dots in a non-polar solvent, such as benzene or diethyl ether, surface modification of the nanoparticles is required. The only solvents that the C dots cannot be dispersed in are strong acids and bases, which dissolve the silica shell. Additionally, these nanoparticles can resist degradation at temperatures up to 150°C.

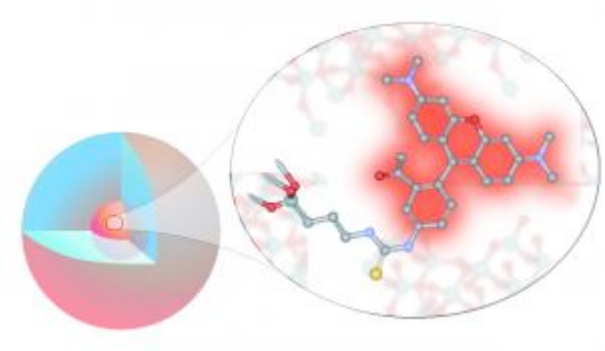

Figure 1. Structure of C dots [17].

In this study, the C dots were incorporated into cellulose acetate (CA) fibers during the fiber spinning process to create an anti-counterfeiting device. Cellulose acetate was used because it is relatively simple to spin, and its acetone solvent is compatible with the C dots. Even though cellulose acetate forms a relatively weak fiber, it is preferable in this experiment because of its low cost and spinnability.

If several different wavelengths of nanoparticles are spun into these CA fibers, and the fibers are arranged in an intricate pattern, an anti-counterfeit device can be made. Recently, a similar anti-counterfeit method has been patented using quantum dots as fluorescent taggants in security inks, papers and explosives [19]. Unfortunately, quantum dots contain heavy metals, such as toxic Cadmium, that have the potential to leak and disrupt the chemistry where the particles are placed [20]. C dots, however, exhibit comparable brightness to quantum dots, but without the

toxicity. In this way, anti-counterfeiting methods utilizing C dots have greater commercial potential than methods using quantum dots.

In this project, the C dots were incorporated into cellulose acetate fibers spun by two distinct methods: electrospinning and dry spinning. These two methods illustrated that the C dots can be dispersed in a nonwoven fabric, or an individual fiber.

Electrostatic fiber spinning or 'electrospinning' is a novel method for forming fibers with submicron scale diameters through electrostatic forces. When an electrical force is applied at the interface of a liquid polymer, a charged jet is ejected. The jet initially extends in a straight line, then moves into a whipping motion caused by the electro hydrodynamic instability at the tip. As the solvent evaporates, the polymer is collected onto a grounded piece of aluminum foil as a nonwoven mat [21].

Dry spinning is a technique commonly used to spin cellulose acetate fibers, and is a common industrial spinning method. The dope solution is composed of cellulose acetate-acetone mixture with approximately 15-30 wt% of the polymer. The dope solution is extruded from a spinneret, and the solution is drawn down to a roller at the bottom of the spinning column [22].

Through the formation of nanoparticle-containing fibers through electrospinning and dry spinning, an anti-counterfeiting device was created. The results of this research show that it is possible to create a unique method for tagging and identifying legitimate items using fluorescing nanoparticles and CA fibers.

MATERIALS AND METHODS

Materials

Cellulose acetate (M_w = 30,000 and M_w = 50,000) was supplied by Aldrich Chemical Co Ltd (St. Louis, MO). Acetone was purchased from VWR Scientific

(West Chester, PA). The C dots were made by the Wiesner lab in the Materials Science and Engineering department at Cornell University.

Preparation of electrospun and dry spun solutions

The electrospun fabrics were manufactured using cellulose acetate (M_w = 30,000), and the dry spun fibers were formed with M_w = 50,000 cellulose acetate (CA). Both CA solutions were composed of a 3:1 ratio of acetone to water. The C dots were suspended in acetone, and added to the CA solutions in 5, 10, 15 vol%, which resulted in 21, 22, 23 wt% in the fiber after solvent evaporation. The mixture of cellulose acetate, acetone, water and C dots were mixed on an Innova™ 2300 platform shaker (New Brunswick Scientific Co., NJ) for twenty-four hours, and then spun through their respective methods.

Electrospinning

The electrospinning apparatus consisted of a programmable syringe pump (Harvard Apparatus, MA) and a high-voltage supply (Gamma High Voltage Research Inc., FL). Electrospinning required a 17 wt% concentration of the lower molecular weight CA, and was spun from a 20 G needle at 0.3 ml/hr with an applied voltage of 14 kV. The nonwoven fabric was formed on a grounded aluminum collector 15 cm from the spinneret tip. The fabric was air dried for approximately 2 hours before storage in a desiccator.

Dry Spinning

Dry spinning was performed using a dry spinning apparatus produced by Alex James & Associates, Inc., Greer, SC. The higher molecular weight concentration of

CA was used for this purpose; a 17 wt% solution was spun and drawn onto a spindle. The fibers were air dried for approximately 2 hours prior to storage in a desiccator.

Thermogravimetric Analysis

A TGA 2050 from Texas Instruments was used to determine the actual weight percent of nanoparticles that were spun into the CA fibers. Both the electrospun and dry spun fibers were heated from 25°C to 400°C at a step rate of 20°C per minute.

Confocal Microscopy

A Leica TCS SP2 laser confocal scanning microscope was used to examine the visible fluorescence of the C dots within the cellulose acetate fibers. The electrospun fabrics were imaged dry at 40X, while the single dry spun fibers were imaged in oil at 40X.

Scanning Electron Microscopy

Morphology and fiber diameter for the electrospun and dry spun fibers was examined using a Leica 440 scanning electron microscope (SEM) at 25 kV and 30 kV. The dry spun samples were imaged under 25 kV, while the electrospun samples were imaged under 30 kV with an electron backscatter detector. Samples were coated for 30 seconds with Au–Pd to prevent charging.

Mechanical Testing

The mechanical data in this study was compiled using ASTM standards D3822 and D638-02a with the Instron 5566. These standards measure the modulus, tensile stress at break, and tensile strain at break that the CA fibers and fabrics can survive prior to failure. Ten dry spun fiber samples were broken from an initial length of 20

mm at a rate of 100 mm/min. The electrospun mats were initially cut into dumbbells with a 3.18 mm width and 9.53 mm length. These samples were then broken at 100 mm/min. The data was then analyzed using the student's t-test, which was used to determine if the control and nanoparticle-containing samples were statistically different from each other. The control sample was compared to each of the samples containing C dots to determine the influence their incorporation had on the mechanical properties of the fibers and fabrics.

RESULTS AND DISCUSSION

Thermogravimetric Analysis (TGA)

By simple calculation, a sample containing 15 vol% of nanoparticles in a 17 wt% solution of CA should contain 47 wt% of nanoparticles within the final fiber. TGA was used to verify the final concentration of nanoparticles within the CA fibers after spinning. However, the TGA data indicated that the actual amount of nanoparticles within the fibers was substantially lower than estimated. The electrospun samples, which should have contained 23, 37, 47% C dots, actually contained 21, 22, 23% C dots, respectively (Figure 2). TGA analysis of the dry spun samples gave inconsistent values, ranging from 5-37% C dots. A sample of one TGA trial for the dry spun samples can be seen in Figure 3. We believe that the dry spinning method lead to these inconsistencies, therefore it was difficult to accurately measure the final weight percent of nanoparticles using TGA due to sample-to-sample variation. The TGA measurements confirmed that distribution of C dots within the dry spun fibers was non-uniform, with some lengths of fibers containing significantly greater C dots loading than other lengths within the same sample. Therefore, on

average, the dry spun fibers were estimated to contain similar quantities of nanoparticles as the electrospun samples: 21, 22, 23% C dots.

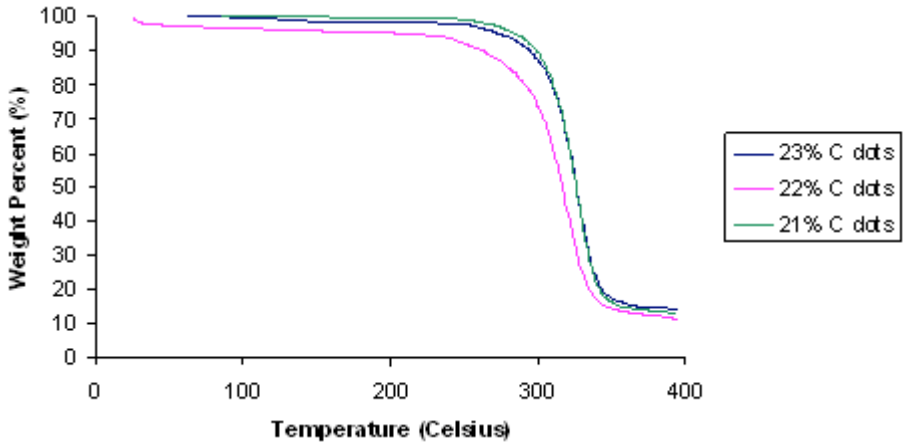

Figure 2. TGA data for the electrospun samples containing 21, 22, 23% C dots.

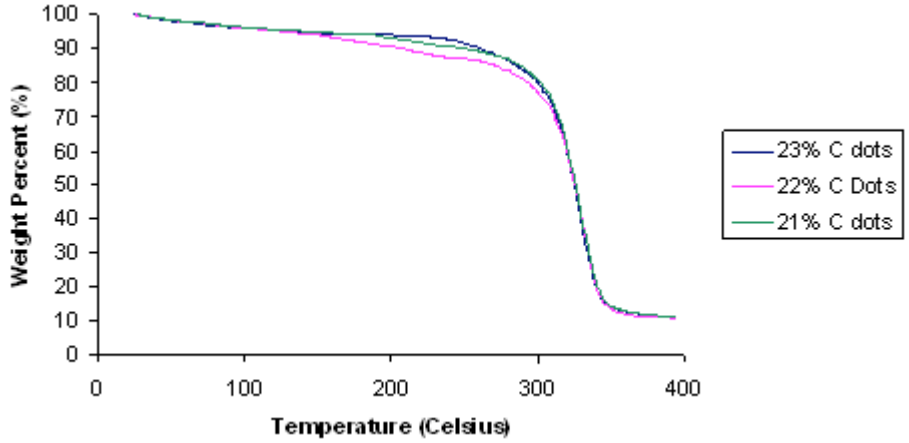

Figure 3. TGA data for the dry spun samples containing 21, 22, 23% C dots.

Confocal and SEM Images

The most conclusive data relevant to this study was seen in the confocal and scanning electron microcopy images, which confirmed the successful incorporation of the C dots in both electrospun and dry spun CA. These confocal images showed that

the nanoparticle-containing fibers appeared white under visible light, and fluoresced under fluorescent light, which confirmed that neat CA fibers did not fluoresce at the target wavelength. The SEM images were used to examine the morphology of the fibers, provide evidence of C dot agglomeration within fibers, and to determine the average fiber diameters. A summary of the electrospun fiber diameters can be seen in table I. The electrospun nanoparticle-containing samples were imaged under an SEM with an electron backscatter detector (EBSD) and an accelerating volatage of 30 kV. The increased accelerating voltage allowed the EBSD to show differences in atomic mass within the fibers through contrast. In this study, a contrast between the silica nanoparticles, and CA was desired.

Representative confocal and SEM images of neat CA fibers prepared by electrospinning and dry spinning are presented in figures 4 and 5. The confocal images are completely black, which clearly showed that CA does not fluoresce at 488 nm light (Figures 4a and 5a). Images taken of the same microscopic field under white light confirm that fibers are present (4b and 5b). The average electrospun fiber diameter without nanoparticles was approximately 1.26 microns, with a standard deviation of 0.811 (Figure 4c). The SEM images also illustrated the morphology of the fibers: the electrospun CA fibers were very smooth, with a ribbon shaped cross-section. The dry spun fibers had non-uniform cross-sections, and showed large pores on the fiber surface as a result of solvent evaporation during the spinning process.

Table I. Summary of fiber diameters for the electrospun samples.

	Control	21% C dots	22% C dots	23% C dots
Average Fiber Diameter (μm)	1.257	1.373	1.504	2.416
Standard Deviation	0.811	0.702	0.574	2.082

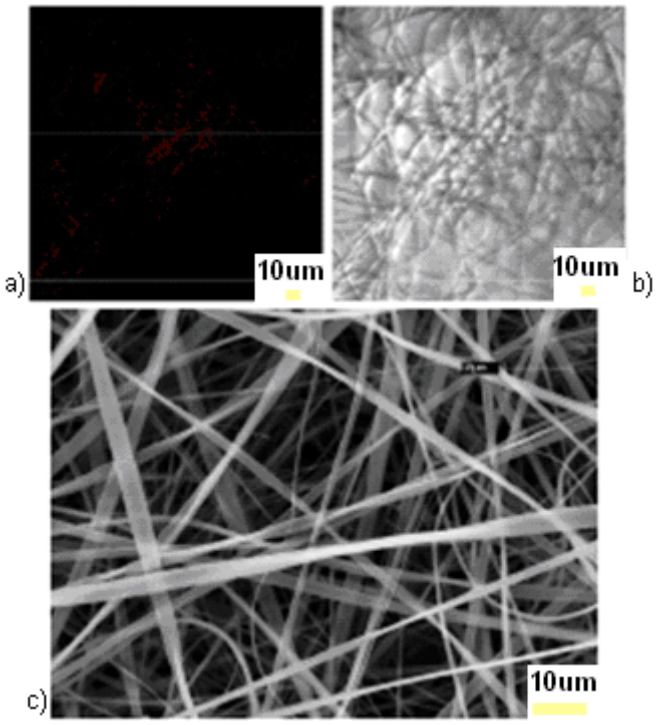

Figure 4. Electrospun sample without C dots under a) confocal microscopy and b) SEM.

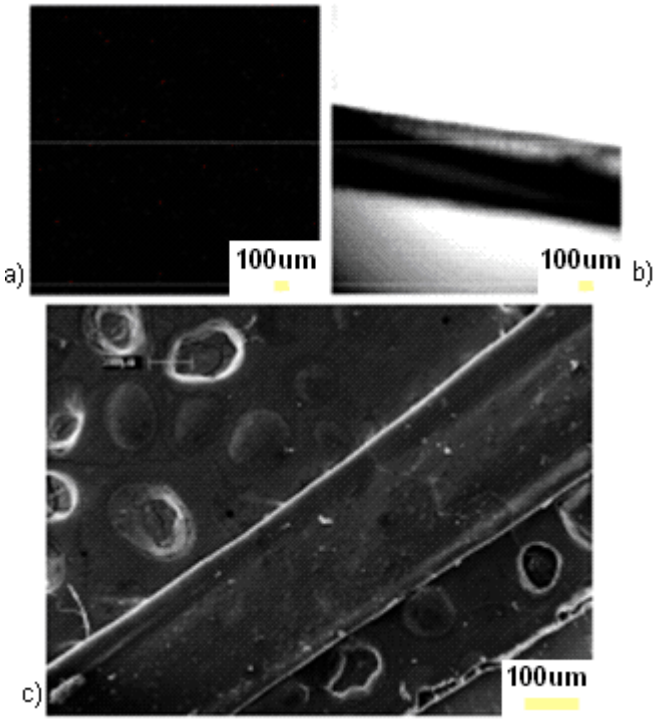

Figure 5. Dry spun sample without C dots under a) confocal microscopy and b) SEM.

Confocal and SEM images of 21 wt% CA fibers prepared by electrospinning and dry spinning are presented in figures 6 and 7. The confocal images show CA fibers uniformly fluorescing under 488 nm light (Figures 6a and 7a). Images taken of the same microscopic field under white light confirm that fibers are present where the fluorescence is observed (6b and 7b). The average electrospun fiber diameter with 21% nanoparticles was approximately 1.38 microns, with a standard deviation of 0.702 (Figure 6c). The SEM images also illustrated the morphology of the fibers: the electrospun CA fibers were very smooth, with a ribbon shaped cross-section. The dry spun fibers had non-uniform cross-sections, and showed large pores on the fiber surface as a result of solvent evaporation during the spinning process. Under the EBSD, only a small number of areas of contrast were observed.

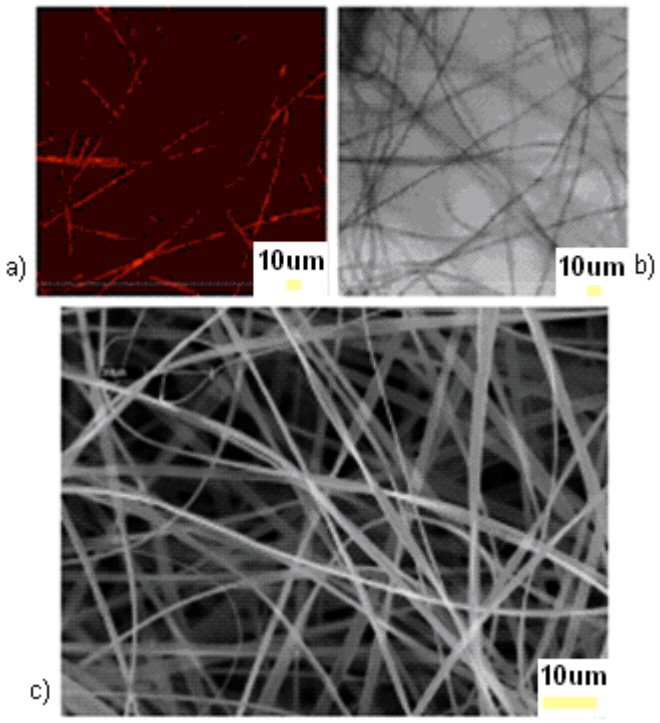

Figure 6. Electrospun samples containing 21% C dots under a) confocal microscopy and b) SEM.

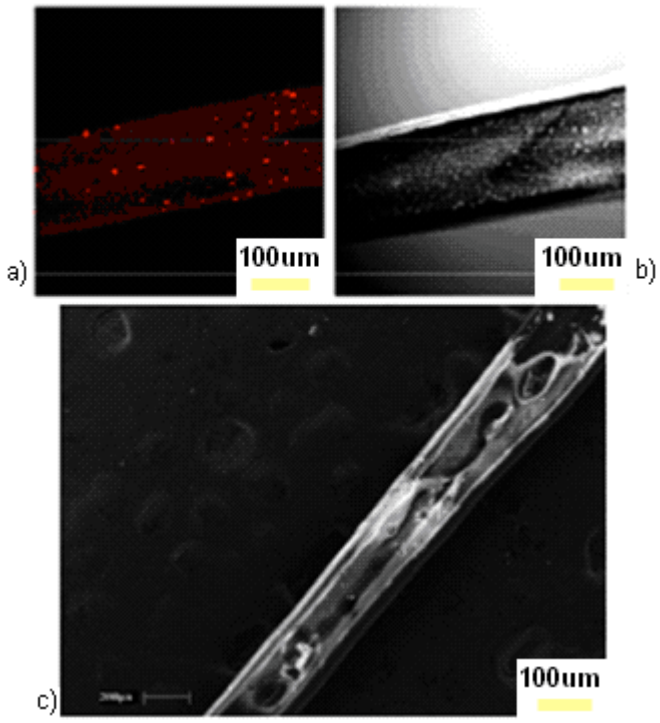

Figure 7. Dry spun sample containing 21% C dots under a) confocal microscopy and b) SEM.

Confocal and SEM images of 22 wt% CA fibers prepared by electrospinning and dry spinning are presented in figures 8 and 9. The confocal images show CA fibers uniformly fluorescing under 488 nm light, the brightness of these fibers was very similar to the 21% C dot samples (Figures 8a and 9a). Once again, images taken of the same microscopic field under white light confirm that fibers are present where the fluorescence is observed (8b and 9b). The average electrospun fiber diameter with 22% nanoparticles was approximately 1.43 microns, with a standard deviation of 0.574 (Figure 8c). The SEM images also illustrated the morphology of the electrospun and dry spun fibers, which was observed to be the same as the control and 21% sample. Under the EBSD, only a small number of contrast points were observed, but more of these contrasting areas were observed than in the 21% sample.

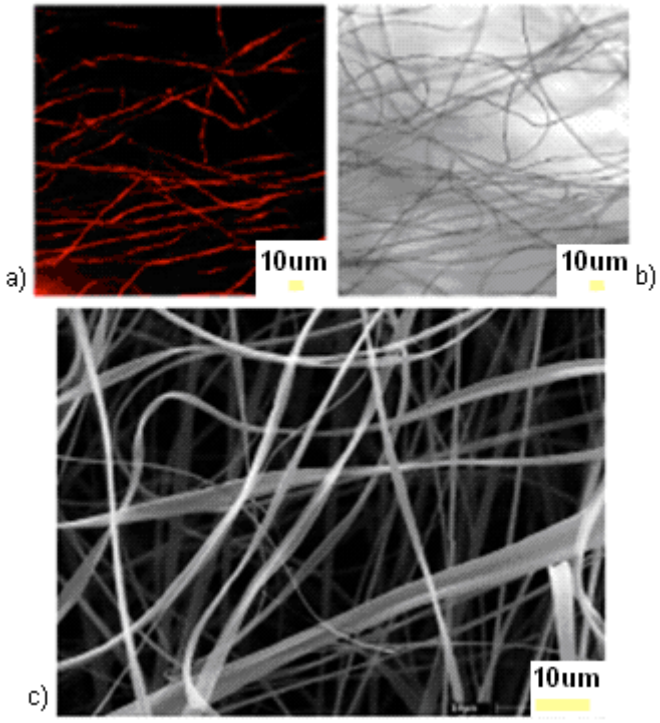

Figure 8. Electrospun sample containing 22% C dots under a) confocal microscopy and b) SEM.

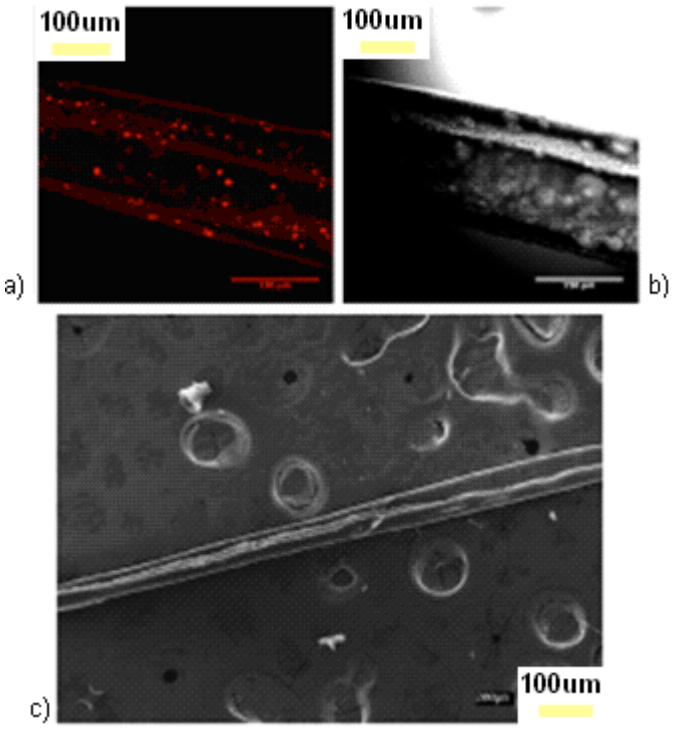

Figure 9. Dry spun sample containing 22% C dots under a) confocal microscopy and b) SEM.

Confocal and SEM images of 23 wt% CA fibers prepared by electrospinning and dry spinning are presented in figures 10 and 11. The confocal images show CA fibers fluorescing, but much of the fluorescence can be seen in bright nanoparticle agglomerates, followed by areas of sparse fluorescence (Figures 10a and 11a). These C dot agglomerations cause the CA fibers to exhibit non-uniform fluorescence. Again, images taken of the same microscopic field under white light confirm that fibers are present where the fluorescence is observed (10b and 11b). The average electrospun fiber diameter with 23% nanoparticles was approximately 2.42 microns, with a standard deviation of 2.08 (Figure 8c). The SEM images also illustrated the morphology of the electrospun and dry spun fibers, which was observed to be the same as the control, 21%, and 22% sample. The only morphological difference between the 23% sample, as compared to the other samples, is a slight increase in fiber diameter. Under the EBSD, several contrast points were observed; many more contrasting areas were observed than in the 21% and 22% samples.

Interestingly, all of the electrospun and dry spun fibers had consistent morphologies. All of the electrospun fibers were very smooth, with only a slight increase in fiber diameter with the 22% sample. The dry spun fibers were all morphologically identical, with the exception of inconsistent diameters due to sample-to-sample variation in the spinning process.

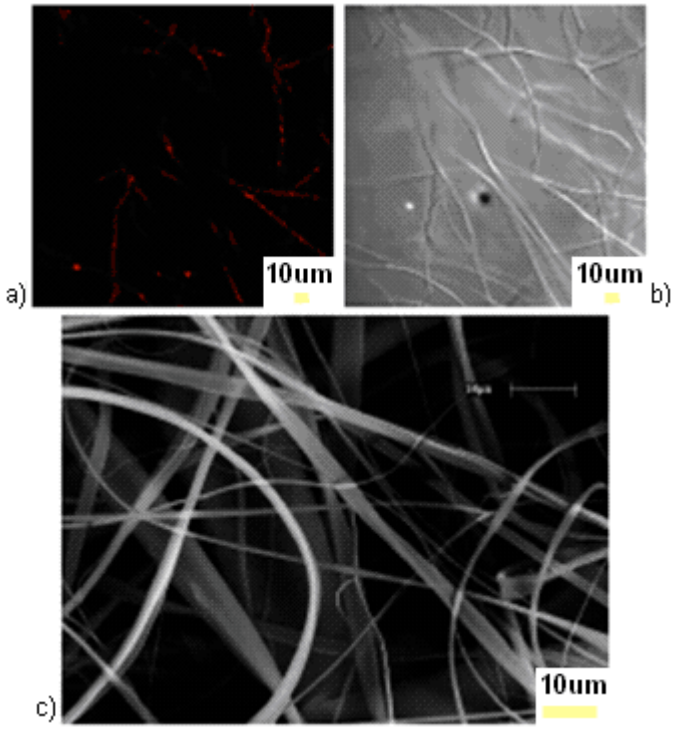

Figure 10. Electrospun sample containing 23% C dots under a) confocal microscopy and b) SEM.

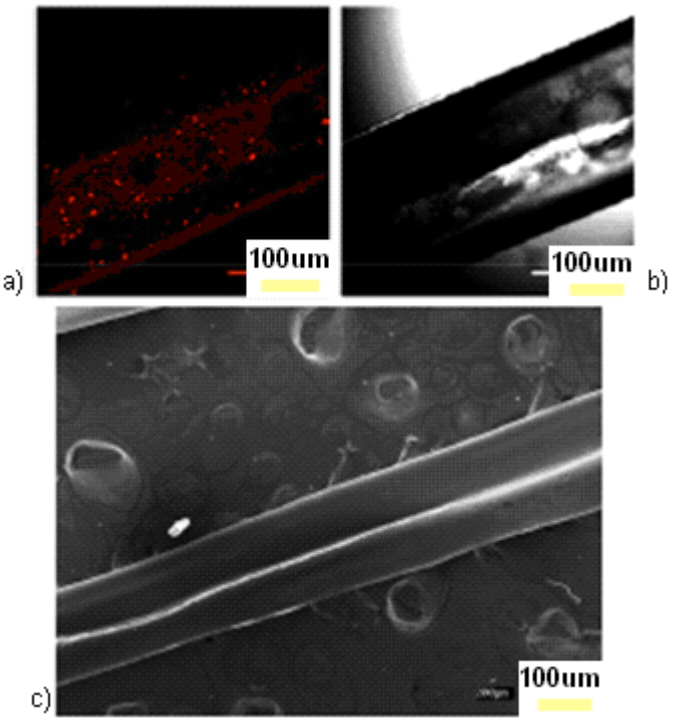

Figure 11. Dry spun sample containing 23% C dots shown under a) confocal microscopy and b) SEM.

Statistical Analysis of Mechanical Testing Data

The mechanical testing data in this study was conducted using ASTM standards D3822 and D638-02a. These standards provide a method to measure the modulus, tensile stress at break, and tensile strain at break that the cellulose fibers and fabrics can survive prior to failure.

Once the mechanical data was compiled, it was necessary to analyze whether the addition of the nanoparticles had any effect on the mechanical properties of the cellulose acetate fibers. Initially, bar charts (Figure 11-13) showed the average values of modulus, tensile stress, and tensile strain for each of the C dot concentrations. Then, a statistical t-test was performed to assess the variability between the control results, and the results of the samples containing varying amounts of C dots (Table II-III). These tests were done under the null hypothesis that there was no significant difference between the values of the control and the C dot containing samples. A percentage of lower than 5% indicated that there was a significant difference between the control values, and the value of the C dot containing samples. Each of the properties are shown and analyzed below.

Table II. Mechanical testing and statistical t-test data for CA electrospun mats normalized by weight.

a) Modulus (GPa/g)

	Control	**21%**	**22%**	**23%**
Average	1.61E-06	1.80E-06	2.46E-06	1.58E-06
Standard Deviation	3.92E-07	5.16E-07	5.21E-07	7.85E-07
T-Test		**22.23%**	**1.74%**	**94.04%**

b) Tensile Stress (MPa/g)

	Control	**21%**	**22%**	**23%**
Average	2.27E-04	2.19E-04	1.88E-04	2.01E-04
Standard Deviation	7.89E-06	1.53E-05	4.65E-05	1.27E-05
T-Test		**79.46%**	**0.82%**	**2.97%**

c) Tensile Strain (%/g)

	Control	**21%**	**22%**	**23%**
Average	1.83E-02	1.63E-02	1.35E-02	1.86E-02
Standard Deviation	5.51E-03	4.48E-03	4.62E-03	4.67E-03
T-Test		**42.91%**	**7.92%**	**99.12%**

Table III. Mechanical testing and statistical t-test data for CA dry spun fibers normalized by weight.

a) Modulus (GPa/g)

	Control	**21%**	**22%**	**23%**
Average	3.92E+04	1.82E+05	9.43E+04	7.89E+04
Standard Deviation	3.03E+04	9.74E+04	3.20E+04	2.69E+04
T-Test		**0.36%**	**0.76%**	**0.62%**

b) Tensile Stress (MPa/g)

	Control	**21%**	**22%**	**23%**
Average	1.80E+03	7.01E+03	3.99E+03	3.72E+03
Standard Deviation	1.36E+03	2.92E+03	2.04E+03	1.63E+03
T-Test		**0.17%**	**4.21%**	**1.93%**

c) Tensile Strain (%/g)

	Control	**21%**	**22%**	**23%**
Average	1.21E+03	1.57E+03	1.14E+03	1.27E+03
Standard Deviation	3.64E+02	6.71E+02	4.61E+02	4.69E+02
T-Test		**8.98%**	**73.24%**	**66.06%**

Electrospun Samples

The modulus of the electrospun control sample was statistically similar to those of the 21% and 23% samples. However, the modulus for the 22% sample was significantly higher than the control, as well as the 21% and 23% samples. The t-test confirmed this result, rejecting the null hypothesis that there was no significant difference between the modulus of the control, as compared to the modulus of the 22% sample (Figure 12a).

The tensile stress at break was statistically similar for the electrospun control and 21% sample. However, the 22% and 23% sample showed an average tensile stress at break that was significantly lower than the control and 21% sample. It appears that the fabric tensile stress can increase with a small amount of nanoparticle loading, but decreases with any additional amount. The t-test confirmed this result, both the 22% and 23% samples had tensile stresses at break that were significantly different to those in the control and 21% sample (Figure 12b).

The tensile strain at break for the electrospun mats did not appear to be affected by the addition of the nanoparticles. The values for tensile strain at break for the control samples were not significantly different than the values compiled for the samples containing 21%, 22%, 23% C dots. The control and 23% samples had statistically identical values for tensile strain, while the 21% and 22% samples were slightly lower. The t-test confirmed that there was no significant difference between the values of tensile strain at break among the samples (Figure 12c). The addition of the C dots did not affect the tensile strain at break for the nonwoven fabrics.

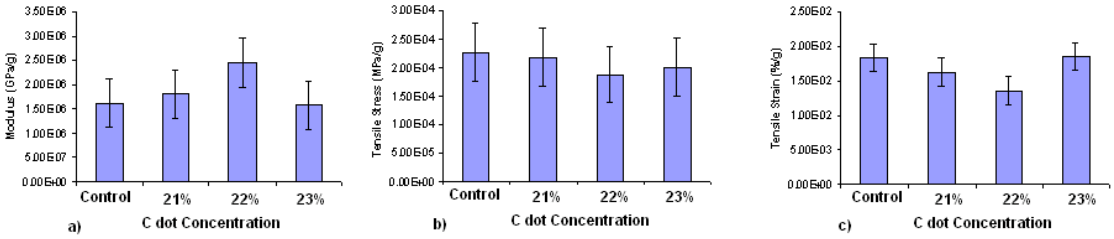

Figure 12. Bar graph illustrating the a) average moduli b) average tensile stress at break and c) average tensile strain at break for electrospun CA fibers.

Dry Spun Samples

The modulus of the dry spun control sample was significantly less than the moduli of the 21%, 22% and 23% samples. The data appeared to show that the presence of the nanoparticles increased the moduli of the dry spun fibers. The t-test confirmed this result, rejecting the null hypothesis that the mean values for the control were similar to the values of the samples containing the nanoparticles (Figure 13a). The addition of the C dots lead to an increase in modulus.

Interestingly, the data for tensile stress at break for the dry spun fibers was statistically similar to the moduli data for dry spun fibers. The tensile stress at break increased significantly with the addition of the nanoparticles. Even though the 21% samples show the greatest increase in tensile strength, the 22% and 23% samples both show values greater than the control sample. Once again, the t-test rejected the null hypothesis that the addition of nanoparticles did not change the tensile stress at break (Figure 13b). The addition of the C dots lead to an increase in tensile stress at break.

Similarly, the tensile strain at break for the dry spun fibers did not appear to be affected by the addition of the nanoparticles. Once again, the tensile strain showed a maximum at 21% loading, but all of the other samples exhibited comparable values to that of the control (Figure 13c). The addition of the C dots had no effect of the tensile strain at break.

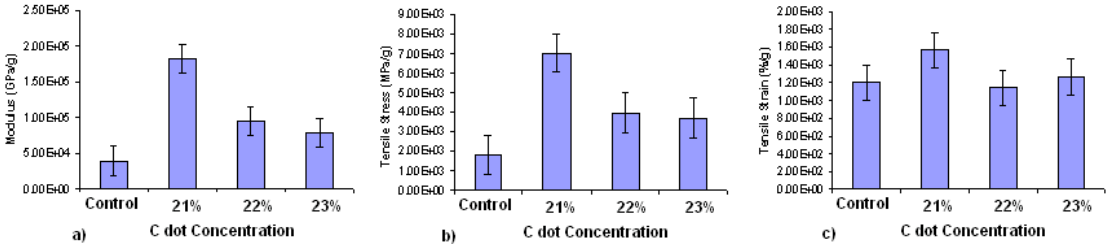

Figure 13. Bar graph illustrating the a) average moduli b) average tensile stress at break and c) averge tensile strain at break for dry spun CA fibers.

CONCLUSIONS

In this study, fluorescent nanoparticles were successfully incorporated into CA fibers for use as an anti-counterfeiting device. Various amounts of nanoparticles were added to both dry spun and electrospun fibers and fabrics. Confocal microscopy confirmed that these nanoparticles fluoresce within the fiber at a specific wavelength of light. SEM images showed that these nanoparticles were successfully incorporated into the fiber. ASTM standards and the statistical t-test were used to assess the mechanical properties of the fibers and fabrics. These tests determined that the addition of nanoparticles affected the modulus and tensile stress values of the 22% and 23% electrospun fabrics. Additionally, the moduli and tensile stress values of the 21%, 22%, and 23% dry spun samples were affected by nanoparticle loading. This research provides sufficient proof that fibers containing fluorescent nanoparticles have the potential to be used as an anti-counterfeiting device.

REFERENCES

1. *First Global Conference in Combating Counterfeiting*. 25 May 2004. <http://www.anticounterfeircongress.org/wco2004/website.asp?page=press>.

2. Hilton, B., Choi, CJ, Chen, S, *The ethics of counterfeiting in the fashion industry: Quality, credence and profit issues*. Journal of Business Ethics, 2004. **55**: p. 344-354.

3. Wong, K., P Hui, and A Chan, *Cryptography and authentication in RFID passive tags for apparel products*. Computers in Industry, 2006. **57**(4): p. 342-349.

4. Yan, E., Cheng Wang, Zonghao Huang, Yi Xin, and Yanbin Tong, *Synthesis and Characterization of 1D Tris(8-Quinilinolato) Aluminum Fluorescent Fibers by Electrospinning*. Materials Science and Engineering, 2007. **464**: p. 59-62.

5. Moreda, G.F.J., Francisco J. Arregui, Miguel Achaerandio, and Ignacio R. Matias, *Study of Indicators for the Development of Fluorescence Based Optical Fiber Temperature Sensors*. Sensors and Actuators B: Chemical 2006. **118**: p. 425-432.

6. Yu, H., Alexander Argyros, Geoff Barton, Martijn Van Eijkelenborg, Christopher Barbe, Kim Finnie, Linggen Kong, Francois Ladouceur, and Scott

McNiven, *Quantum Dot and Silica Nanoparticle Doped Polymer Optical Fibers*. Optics Express, 2007. **47**: p. 9989-9994.

7. Radojevic, V.N., D; Talijan, N; Trifunovic, D; Aleksic, R, *Optical fibers with composite magnetic coating for magnetic field sensing*. Journal of Magnetism and Magnetic Materials, 2004. **5**: p. 272-276.

8. Xianfeng, L.Y., Zha;, Ce, Wang, *Fabrication of PbS nanoparticles in polymer-fiber matrices by electrospinning*. Advanced Materials, 2005. **17**(20): p. 2485-2488.

9. Bayindir, M., Ayman Abouraddy, Jerimy Arnold, John Joannopoulos, Yoel Fink, *Thermal-Sensing Fiber Devices by Multimaterial Codrawing*. Advanced Materials, 2006. **18**: p. 845-849.

10. Garito, A.F.H., Yu-Ling; Gao, Renyuan; Gao, Renfeng, *Thermal polymer nanocomposites*, U.P. Office, Editor. 2003.

11. House, D.W., *Electrically conducting polymers*, U.P. Office, Editor. 1985.

12. Dhawan, A., Abdelfattah Seyam, Tushar Ghosh, John Muth, *Woven fabric-based electrical circuits: Part 1: Evaluating interconnect methods*. Textile Research Journal. , 2004. **74**(10): p. 913-919.

13. Boen, B., *Not-So-Heavy Metal: Electrical Conductivity in Textiles*, in *NASA Spinoff*. 2007.

14. Coyle, S.W., Y.; King-Tong, L.; Brady, S.; Wallace, G., Diamond, D. *Bio-sensing textiles – wearable chemical biosensors for health monitoring."* in *4th International Workshop on Wearable and Implantable Body Sensor Networks* 2007. Aachen University.

15. Coyle, S., *Chemical Sciences- Adaptive Sensors Group*. 2007. <http://www.dcu.ie/chemistry/asg/coyleshi/>

16. *Firewall Protection for Paper Documents*, in *RFID Journal*. 2007.

17. *CU Dots*. Cornell University. <http:www.news.cornell/stories/May05/Cudots.ws.html>

18. Ow, H., D Larson, M Srivastava, B Baird, W Webb, and U Wiesner, *Bright and Stable Core-Shell Fluorescence Silica Nanoparticles*. Nano Letters, 2005. **5**(1): p. 113-117.

19. *Quantum Dots*, Evident Tech. 11 Jan. 2007 <http://www.evidenttech.com/applications/quantum-dot-ink.php>

20. McGrew, S., *Quantum dot security device and metho*, U.P. Office, Editor. 2004.

21. Kim, C.K., D S. Kim, S Y. Kang, M Marquez, and Y L. Joo, *Structural Studies of Electrospun Cellulose Nanofibers*. Polymer, 2006. **47**(14): p. 5097-5107.

22. Sano, Y., *Drying Behavior of Acetate Filament in Dry Spinning*. Drying Technology, 2001. **19**(7): p. 1335-1359.